

Supporting information

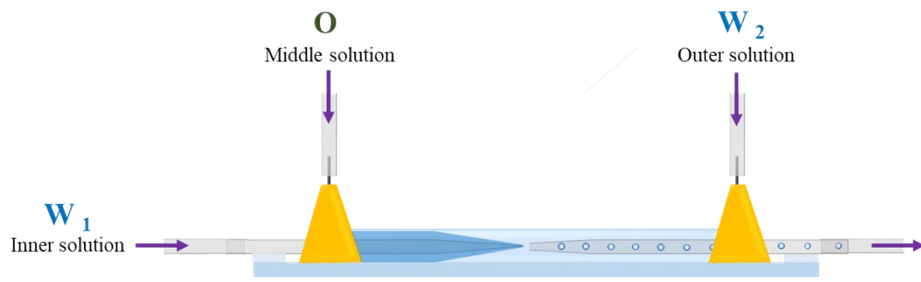
General method for production of hydrogel droplets from uniformly sized smart shell membranes

So-Jeong Gwon and Soo-Young Park*

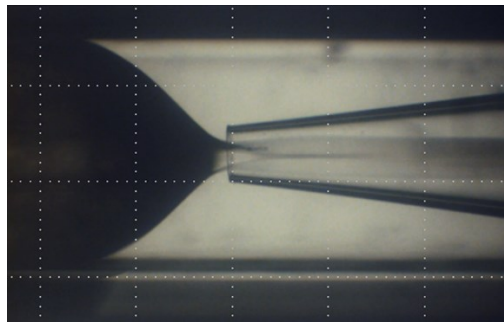
Department of Polymer Science & Engineering, Polymeric Nanomaterials Laboratory,
School of Applied Chemical Engineering, Kyungpook National University, 80 Daehak-ro,
Buk-gu, Daegu 41566, Korea

*E-mail: psy@knu.ac.kr

Text S1 A microcapillary device, comprising round glass capillaries enclosed within a square glass capillary, was used to prepare nematic liquid crystal shells using mixtures of 4-cyano-4'-pentylbiphenyl (5CB) and a reactive mesogen mixture (RMM727). The outer diameter of the round glass capillaries (0.87 mm) was similar to the inner diameter of the square glass capillary (0.9 mm) such that a round glass capillary could be inserted into the square glass capillary from each end to achieve a tight-fitting and coaxial alignment. The tapered ends of the two capillaries were adjacent at the center of the square glass capillary (Fig S1). The diameters of the left and right tapered ends were 70 ± 10 and 250 ± 20 μm , respectively. For preparing RMM/5CB shells, the inner aqueous phase was flowed through the left capillary; further, the RMM/5CB mixture was flowed through the same direction in the square glass capillary, and the outer continuous aqueous phase was flowed through the opposite direction. The RMM/5CB mixture was heated to a temperature greater than the isotropic temperature (70 $^{\circ}\text{C}$) to reduce the viscosity of the dispersed phase. Droplets of the inner aqueous phase were formed within the isotropic phase because the streams of the two co-flowing fluids were disrupted owing to Rayleigh instability. The RMM/5CB mixture and the continuous aqueous phases met between the ends of the two round glass capillaries. Further, the RMM/5CB shells were produced in an isotropic state at the junction but became nematic in the collecting right round glass capillary. The flow rates were controlled using a pneumatic microfluidic flow-rate control system (OB1 MK3, pressure and vacuum controller, Elveflow), which can pump three fluids at three different velocities. This system was connected to a microcapillary device using shrinkable connector tubes and flexible plastic tubing (Norton, inner diameter: 0.51 mm and outer diameter: 1.52 mm). By pumping nitrogen gas at a finely controlled rate into the pressurized reservoir holder rack containing liquids, the OB1 unit pressurized the reservoir, causing the fluids to flow through the tubes and into the device. Three pressures were controlled to get uniformly sized LC shell in microfluidics. P_1 , P_2 , and P_3 represent the pressures of the inner (SDS aqueous solution), middle (RMM), and outer (SDS aqueous solution) fluids, respectively. In order to control size, the P_3 was controlled from 1.0 to 1.8 mbar with fixed pressures of P_1 and P_2 at 1 and 2 mbar, respectively. Figure * shows the optical microscopy images of the glass capillaries during producing LC shells using microfluidics at $P_3 = 1.0, 1.2, 1.4, 1.6$ and 1.8 mbar and the produced LC shells. The outer diameters (and thickness) of the LC shells are 169.8 ± 4.3 (9.5 ± 0.3), 128.7 ± 0.5 (7.0 ± 0.3), 120.8 ± 0.5 (6.4 ± 0.3), 103.5 ± 0.8 (6.2 ± 0.3) and 90.6 ± 0.8 (6.1 ± 0.3) μm at $P_3 = 1.0, 1.2, 1.4, 1.6$ and 1.8 mbar, respectively. The outer diameter decreases as P_3 increases without much change of the thickness. The standard deviation for all LC shells are small, indicating that the size of the LC shells were uniformly controlled by at P_3 ; the diameter and standard deviation were calculated with 30 LC shells. Similarly, the P_1 was controlled from 0.8 to 1.1 mbar with fixed pressures of P_2 and P_3 at 2 and 1.2 mbar, respectively to control the thickness of the LC shell. The shell thicknesses (and outer diameters) of the LC shells were 22.6 ± 2.8 (170.1 ± 2.9), 16.5 ± 0.2 (164.1 ± 0.4), 12.2 ± 0.4 (164.2 ± 0.4), and 10.3 ± 0.5 (167.2 ± 0.3) μm at $P_1 = 0.8, 0.9, 1.0,$ and 1.1 mbar, respectively; the diameter and standard deviation were calculated with 30 LC shells. The thickness decreases as P_1 increases without changing diameter much, indicating that the thickness can be controlled by P_1 with similar out diameters. Thus, we found that diameter and thickness can be easily controlled by the pressures of outer and inner fluids.

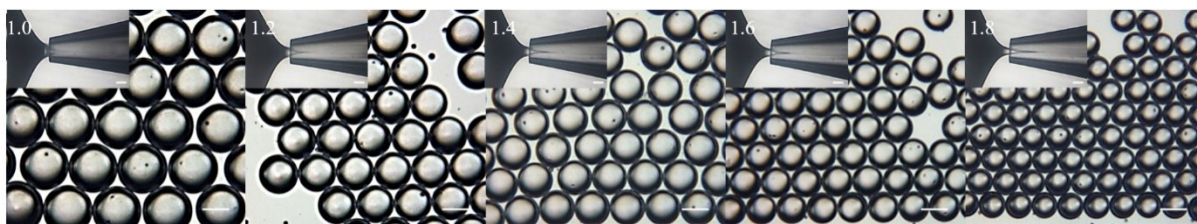


(a)

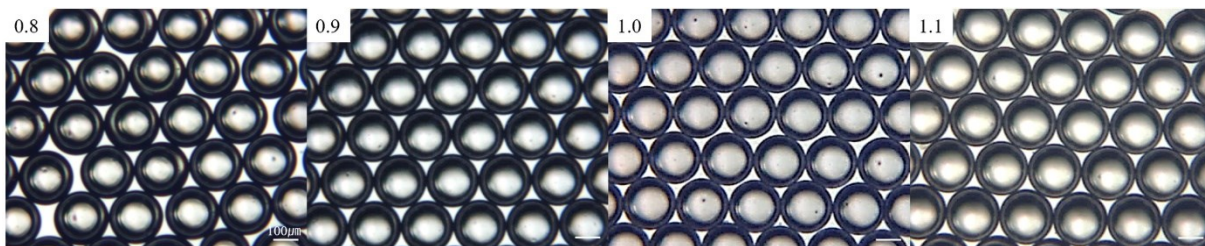


(b)

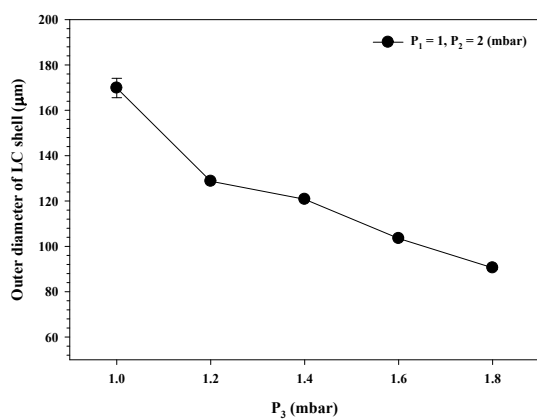
Fig S1 (a) Schematic and (b) photographic images of the glass capillaries having combined flow focusing and co-flow geometries used to produce LC shells.



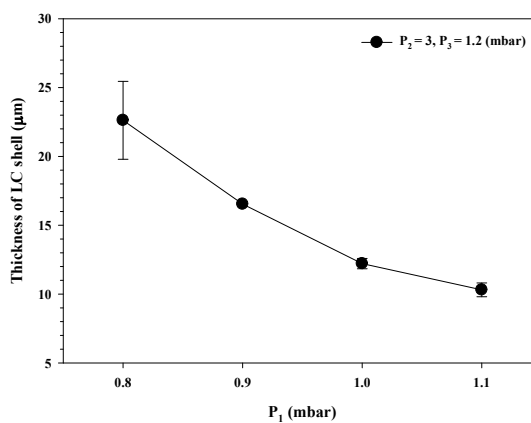
(a)



(b)



(c)



(d)

Fig S2 Optical microscopy images of the LC shells produced at (a) $P_3 = 1.0, 1.2, 1.4, 1.6,$ and 1.8 mbar with $P_1 = 1$ mbar and $P_2 = 2$ mbar with insets of the photographic images of the glass capillaries during producing LC shells using microfluidics, and (b) $P_1 = 0.8, 0.9, 1.0,$ and 1.1 mbar with $P_2 = 3$ mbar and $P_3 = 1.2$ mbar; numbers in (a) and (b) represents P_3 and P_1 , respectively. (c) Measured average outer diameter of LC shell as a function of P_3 (data from (a)), and (d) measured thickness of the LC shell as a function of P_1 (data from (b)) with ~ 30 LC shells; error bars represent the standard deviation.

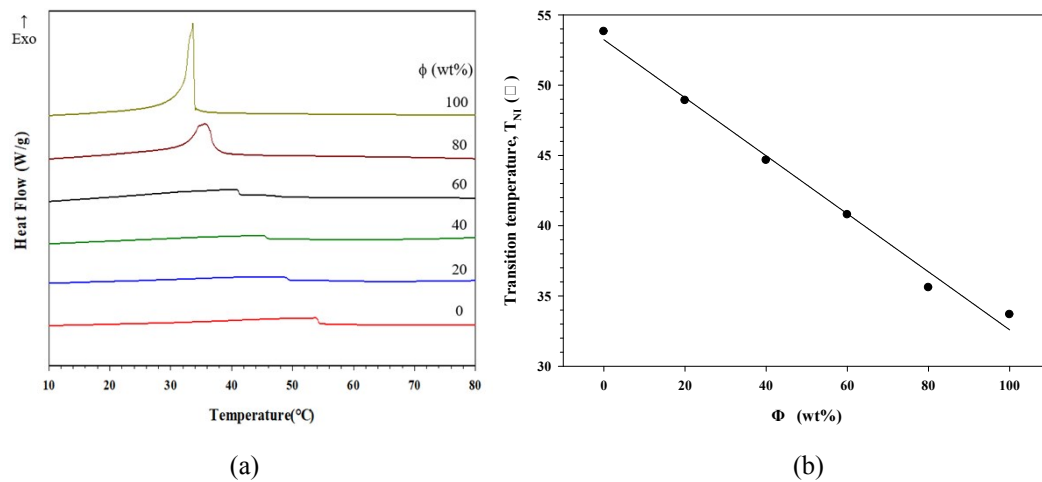


Fig S3 (a) DSC cooling thermograms of the RMM/5CB mixtures at different ϕ values and (b) the nematic to isotropic transition temperature (T_{NI}) of the RMM/5CB mixture as a function of ϕ .

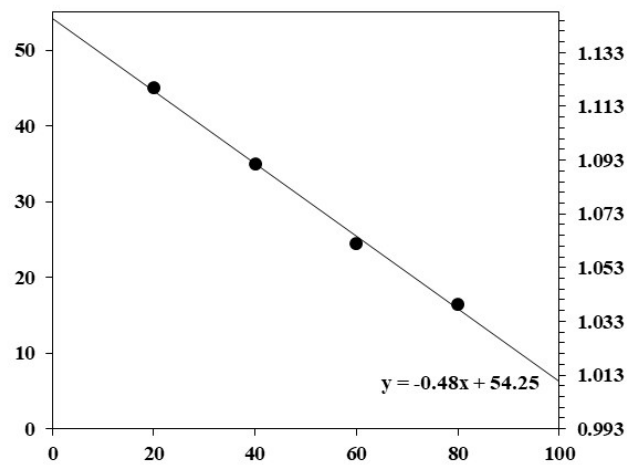
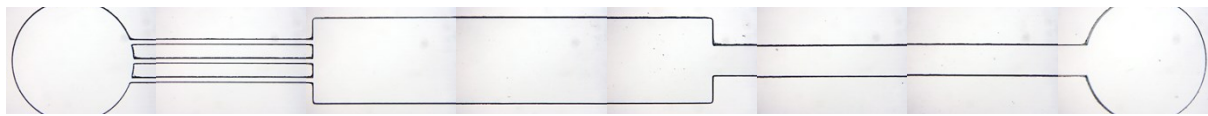
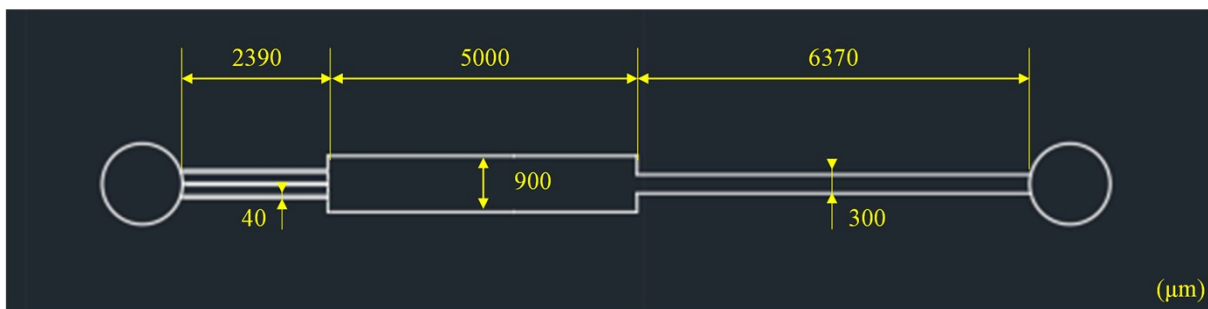


Fig S4 Density of the RMM/5CB mixture as a function of the 5CB content (ϕ).



(a)



(b)

Fig S5 (a) Photographic image of the PDMS chip for storage of PAA droplets and (b) its schematic with the dimensions of the used PDMS chip having an inlet, an outlet, and a storage chamber for PAA droplets as well as outlet channels.

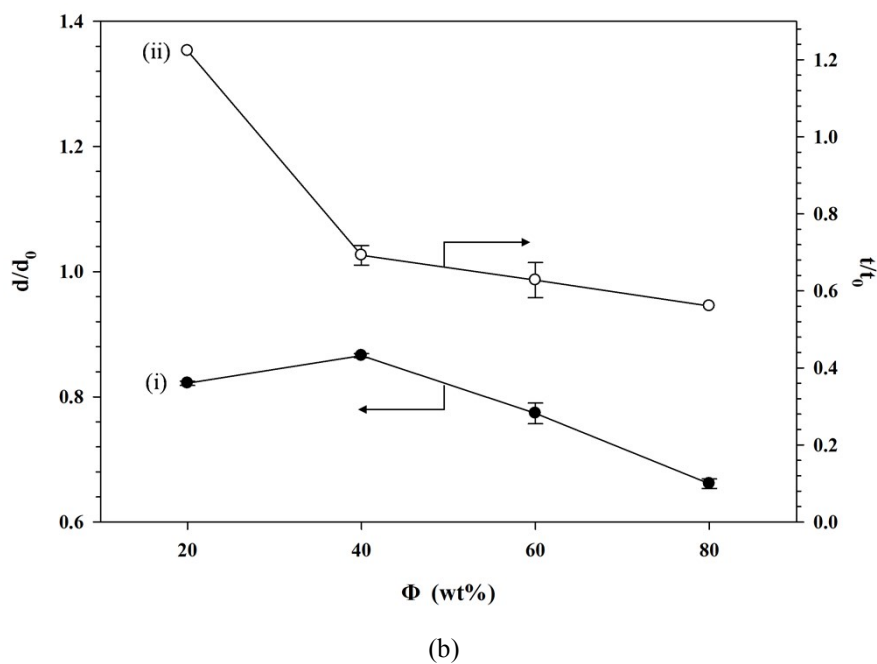
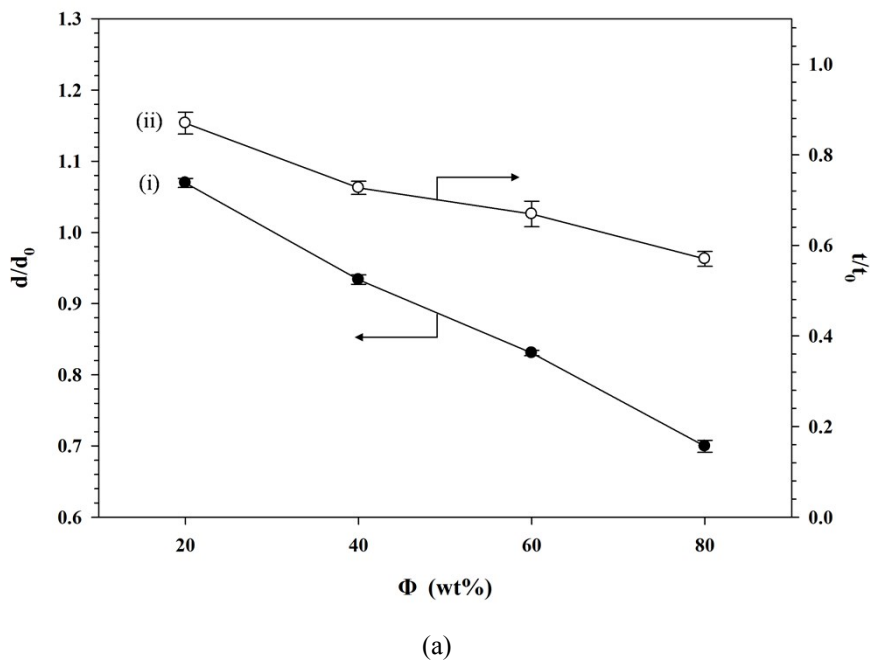


Fig S6 (i) Diameter ratio (d/d_0) (filled circle) and (ii) thickness ratio (t/t_0) (open circle) of the LC_{solid} shell in (a) acetone and (b) water as a function of ϕ , where d_0 (t_0) and d (t) are the outer diameters (thicknesses) of the shell before and after 5CB extraction, respectively; the diameter and thickness are averaged using 30 LC_{solid} shells, and error bars represent the standard deviation.

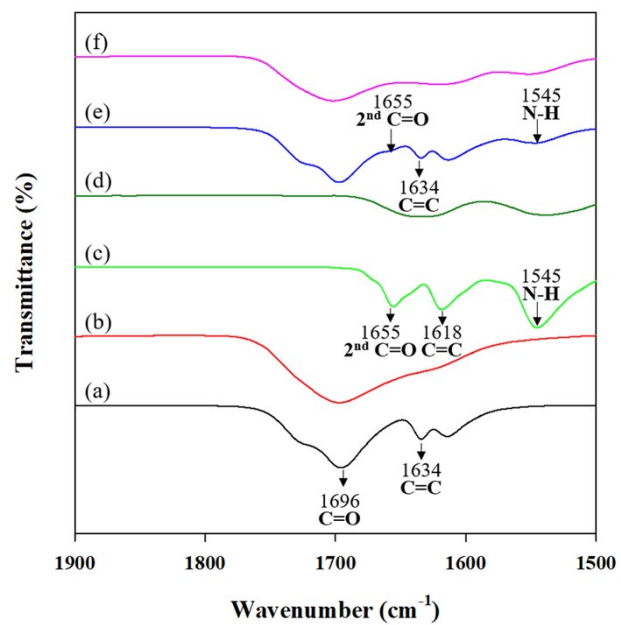


Fig S7 FTIR spectra of (a) AA, (b) PAA, (c) NIPAM, (d) PNIPAM, (e) AA/NIPAM (9:1 mole ratio), and (f) P(AA-co-NIPAM) (9:1 mole ratio).

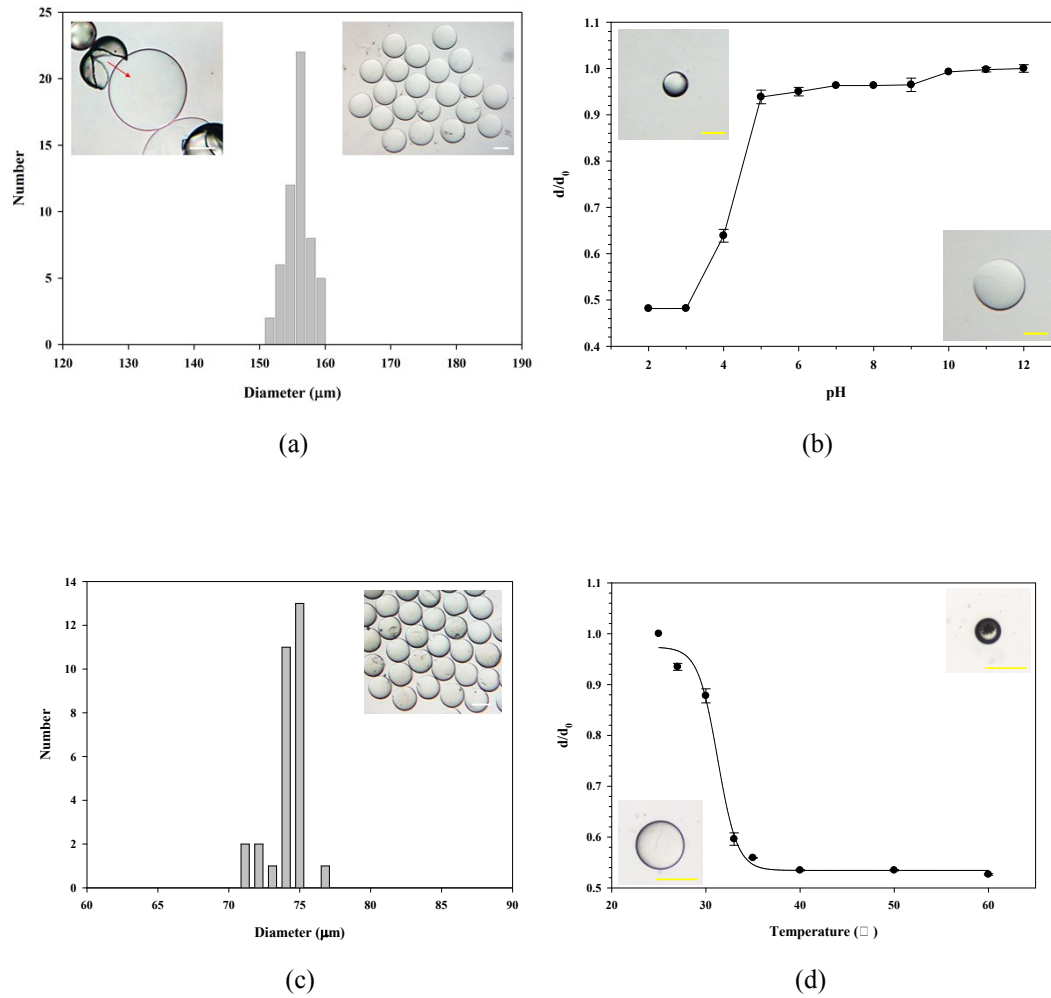


Fig S8 (a) Size distribution of the crosslinked PAA hydrogel droplets based on the optical microscopy images of the packed droplets (right inset) and the process of escaping from the LC_{solid} shells (left inset). (b) Diameter ratio (d/d_0) of the crosslinked PAA hydrogel droplets as a function of pH with a reference diameter (d_0) at pH = 12. (c) Size distribution of the crosslinked P(NIPAM) hydrogel droplets based on an optical microscopy image. (d) Diameter ratio (d/d_0) of the crosslinked P(NIPAM) droplets as a function of the temperature with respect to a reference diameter (d_0) at 25 °C.